

Neutron Diffraction Study of the Structure of Liquid Water

Norio OHTOMO* and Kiyoshi ARAKAWA

Research Institute of Applied Electricity, Hokkaido University, Sapporo 060

*Faculty of Engineering, Hokkaido University, Sapporo 060

(Received October 28, 1977)

The structure factor for heavy water at 17 °C up to the Q value of 18 Å⁻¹ has been determined by means of the time-of-flight (TOF) diffraction method using pulsed neutrons produced by LINAC. The result has been compared with structure factors calculated on the basis of the various structure models of liquid water; the "uncorrelated orientation model" and the "watery model" (Page and Powles), the "near-neighbor model" (Narten) and the "revised watery model" (authors). None of these models has been found to fit the neutron diffraction data satisfactorily over the entire range of Q , though our curve is somewhat improved in comparison with the curves for earlier models. Some discussions about the various structure models of liquid water have been made.

The neutron diffraction method has proved to be a powerful means for the determination of the structure of liquids for these two decades, and its applications into the studies of the structure of liquid water have been carried out since those by Brockhouse¹⁾ and by Springer *et al.*²⁾ Recently, two remarkable studies of the liquid structure of water using the method have appeared, which have been given by Page and Powles³⁾ and by Narten,⁴⁾ and further, the structure factors at higher Q values have been reported.^{5,6)} However, the experimental data are still limited at present.

Among these studies the results³⁾ obtained by Page and Powles and those⁴⁾ by Narten are the most important and interesting from the view-point of the liquid structure of water. The observed structure factors obtained by both of them are found to be not so different from each other, but their conclusions on the structure models of water are largely inconsistent. It has been reported by Narten that the calculated structure factor curve based on his "near neighbor model" is in very good agreement with his observed one. However, because several arbitrarily adjustable parameters are used in his analysis, the physical reality of the model is obscured. On the other hand, any of the structure models treated in Page and Powles' paper has not fitted the diffraction data over the whole range of Q (up to the Q value of 10 Å⁻¹) and has been disproved by them.

Thus, in order to elucidate the structure of liquid water, the authors have carried out a study by the TOF diffraction technique using the electron linear accelerator as a neutron source, which has been developed recently and has turned out to be more favorable for diffraction studies of liquids than that using a reactor as the source.⁷⁾

Experimental

i) *Apparatus and Procedures.* In the TOF diffraction method the analyzing actions are performed by the TOF technique, where the time-of-flight, t [μs] is measured for neutrons of various magnitudes of wavelength λ [Å] at a fixed angle 2θ [degree].⁸⁾ The momentum transfer is $\hbar Q$ and the magnitude of Q becomes

$$Q = \frac{4\pi}{\lambda} \sin \theta = 3177 \frac{L_0 + L}{t} \sin \theta, \quad (1)$$

where L_0 [m] and L [m] is the flight path of the incident and scattered neutron beam, respectively. \hbar is $h/2\pi$ and h is Planck constant. The schematic diagram of the apparatus is shown in Fig. 1.

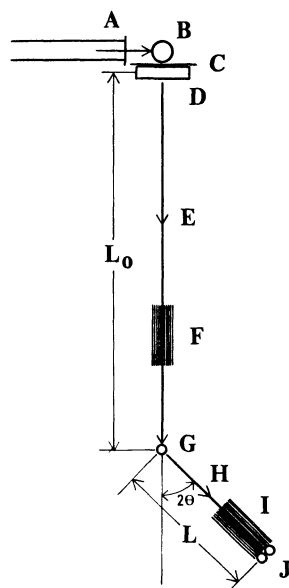


Fig. 1. Schematic diagram of the apparatus.

A: Pulsed electron beam, B: Pb target, C: Cd sheet, D: H₂O moderator assembly, E: incident neutron beam, F: Soller collimator, G: sample, H: scattered neutron beam, I: Soller collimator, and J: ³He counter.

The measurement has been carried out using a pulsed neutron source which is connected to the electron linear accelerator (LINAC) at the Department of Atomic Engineering, Faculty of Engineering, Hokkaido University. In the LINAC a burst of 45 MeV (the pulse width, 3 μs and the repetition frequency of pulse, 100 pps) impinges on a water-cooled heavy metal target (lead) and pulsed photo-neutrons are produced through the (γ , n) reaction in the target. The neutrons are moderated by a water slab (250 × 250 × 25 mm³) and become low energy neutrons in the Maxwell-Boltzmann distribution.⁹⁾ For the purpose of reducing the widening of pulse width caused by reflected neutrons a Cd sheet is inserted between the target and the water slab. The intensity and pulse width of these low energy neutrons are dependent on the shape, dimension and arrangement of the target and the water slab, and then the neutron source system is optimized for raising up the resolution and accuracy in the present experiment.¹⁰⁾

The pulsed beam of heterochromatic neutrons is scattered isotropically by the sample after passing through a flight tube set in a shielding wall and the neutrons scattered to the direction of the angle 2θ are detected by a counter. The neutron beam is collimated by two Soller collimators composed of

parallel Cd-plated sheets before and behind the sample. The slit width of the Soller collimator governs primarily the resolving power as a spectrometer, and, when the measurement is carried out at a small angle, it should be designed to be narrow enough.

The neutrons scattered by the sample are detected by a ^3He counter and are analyzed by a multi-channel time analyzer. Time analysis is carried out with a channel width of 20 μs and a channel number 512. The lower limit of Q in the present experiment becomes about 1 \AA^{-1} at the scattered angle $2\theta=50^\circ$ with the flight path of 7 m.

ii) *Resolution.* The fractional resolution $\Delta Q/Q$ is expressed as

$$\frac{\Delta Q}{Q} = \left[(\Delta\theta \cot\theta)^2 + \left(\frac{\Delta t}{t} \right)^2 + \left(\frac{\Delta L}{L_0 + L} \right)^2 \right]^{1/2}, \quad (2)$$

where $\Delta\theta$, Δt , and ΔL represent the uncertainties in θ , t , and $L_0 + L$, respectively. $\Delta\theta$ is attributed to the widening of the beam $\Delta\theta_1$, which is determined by the slit width of the Soller collimator, as well as to the widening of the beam along the length of the detector and the sample. $\Delta\theta_1$ in the present Soller collimator becomes about 1.72° and this governs $\Delta\theta/\theta$. Δt is determined from the pulse width of the electron beam τ_p in LINAC, the mean-emission-time at the moderator τ_m and the channel width τ_e in the multi-channel time analyzer. The magnitude of τ_m is determined from theoretical and experimental considerations,¹⁰⁾ which becomes about $1 \mu\text{s}$ at $\lambda=0.3 \text{ \AA}$ and increases about $25 \mu\text{s}$ at $\lambda=1.8 \text{ \AA}$. In the present experiment $\tau_p=3 \mu\text{s}$ and $\tau_e=20 \mu\text{s}$. At small wavelength of neutrons τ_e becomes dominant in Δt . The magnitude of ΔL is calculated from the effective radius of the radiation surface

TABLE 1. THE RESOLVING POWER $\Delta Q/Q$

$\lambda[\text{\AA}]$	$\Delta\theta \cot\theta$	$\Delta L/(L_0 + L)$	$\Delta t/t$	$\Delta Q/Q$
1.8	0.066	0.021	0.017	0.070
0.3	0.066	0.021	0.044	0.082

of the neutron source ($=15 \text{ cm}$) and the diameter of the detector ($=2.5 \text{ cm}$).

The resolving power $\Delta Q/Q$ is given in Table 1 for two magnitudes of wavelength. In addition to the estimation of $\Delta Q/Q$ described above the experimental determination of $\Delta Q/Q$ is also carried out, together with the calibration of Q , through the scattering experiment for polycrystalline samples such as Fe, Zr, Cu, etc. which have clear and known Bragg reflection peaks.

Experimental Results

Scattering measurements have been carried out at 17°C for the sample (99.75% D_2O) which was contained in a vessel of Al foil (100 mm long, 9.0 mm in diameter; 0.017 mm wall thickness) and for a vanadium rod of the same shape and dimension as the sample which was used as a standard and further carried out for the estimation of the contribution of background scattering. In Fig. 2 the count rate time-spectrum (the raw data of the scattering) is given, normalized in burst number of LINAC, where the spectrum for vanadium and that for background are smoothed. The magnitudes of resolution ΔQ are given as triangles along the abscissa axis. The statistical error is smaller than 1.7% in the range of $Q > 2 \text{ \AA}^{-1}$, and becomes about 7% for $Q \approx 1 \text{ \AA}^{-1}$. The effective range of Q in the present experiment is up to 18 \AA^{-1} .

In order to determine the structure factors relevant to the molecular model of liquid, the following contributions to observed values as well as the absolute calibration should be subtracted: the multiple scattering, the absorption, the background counting and the inelastic scattering (the Placzek correction). In the present study, firstly, all data are smoothed according to the least square fitting procedure and, thereafter, the

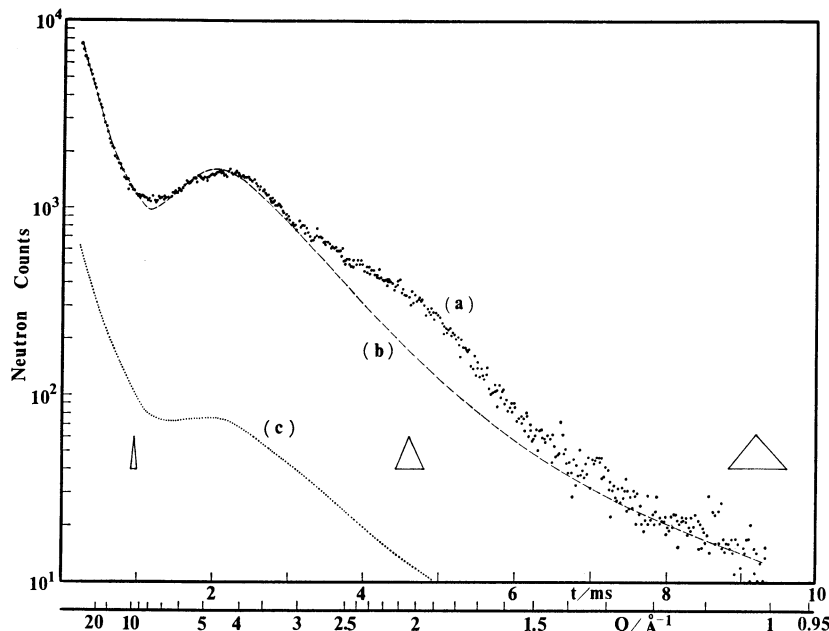


Fig. 2. Time-of-flight spectra.

(a) \bullet : D_2O (17°C) + background, (b) —: vanadium rod + background,
(c): background.

The magnitudes of the instrumental resolution are indicated by triangles at three points.

following corrections and reduction are made for the smoothed spectrum.

a) The multiple scattering correction: Blech and Averbach's method¹¹ has been used for the correction to multiple scattering. The effect of double scattering only is taken into consideration and three or more-fold scattering is ignored. We applied this correction to the scattering data of D_2O and those of vanadium rod.

b) The absorption correction: Paalman and Pings' method¹² has been applied to the absorption correction, which is used as the absorption correction in X-ray analysis for samples and vessels of cylindrical or ring shape.

c) The background correction: The background data shown in Fig. 2 has been subtracted from the scattering data for the sample and the vanadium rod after the application of the multiple scattering and absorption corrections.

d) The Placzek correction: Powles⁶ proposed the method of the Placzek correction for the TOF diffraction method using the LINAC pulsed neutron source. There exist some semiempirical schemes for applying the correction, but any more rigorous numerical procedure applicable over a wide range of Q has not been discovered.¹³ Then, we have applied this method in the present analysis. Page and Powles used 6.7 A.U. as the value of the effective mass M_{eff} ,³ which is the mean mass of the component nuclei of a heavy water molecule. In the present analysis we have used the linearly interpolated values of M_{eff} between 2 A.U. at 20 \AA^{-1} and 20 A.U. at 2 \AA^{-1} . The Placzek correction rises steadily from about 2% at 2 \AA^{-1} to about 8% at 10 \AA^{-1} , and amounts to 16% at 18 \AA^{-1} .

After the application of all corrections the calibration to the absolute cross-section scale has been carried out by comparison of the count rate time-spectrum from the sample D_2O with that from a polycrystalline vanadium rod which is usually regarded as an isotropic and incoherent scatterer. The effect of the corrections described above is seen in Fig. 3 by comparing two

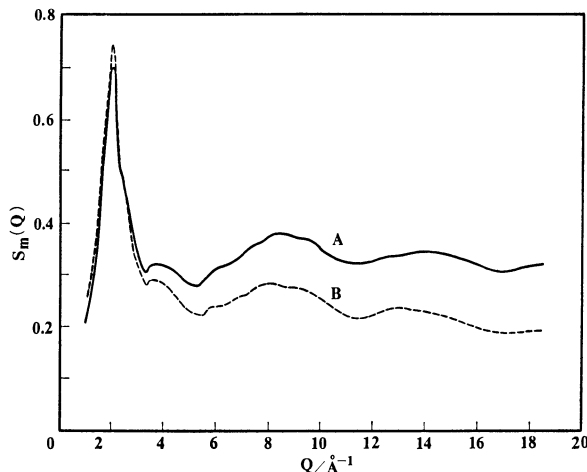


Fig. 3. The effect of the corrections for the observed structure factor $S_m(Q)$.

A: Fully corrected structure factor, B: the background correction only.

TABLE 2. THE OBSERVED ABSOLUTE NEUTRON SCATTERING FACTOR $S_m(Q)$ AS A FUNCTION OF SCATTERING VECTOR Q [\AA^{-1}] FOR HEAVY WATER AT 17 °C

Q	$S_m(Q)$	Q	$S_m(Q)$	Q	$S_m(Q)$
1.0	0.207	4.8	0.287	11.6	0.323
1.1	0.237	5.0	0.284	11.8	0.324
1.2	0.253	5.2	0.279	12.0	0.327
1.3	0.282	5.4	0.277	12.2	0.330
1.4	0.325	5.6	0.291	12.4	0.333
1.5	0.395	5.8	0.300	12.6	0.335
1.6	0.465	6.0	0.309	12.8	0.336
1.7	0.549	6.2	0.316	13.0	0.337
1.8	0.565	6.4	0.317	13.2	0.339
1.9	0.656	6.6	0.324	13.4	0.342
2.0	0.698	6.8	0.331	13.6	0.343
2.1	0.628	7.0	0.339	13.8	0.344
2.2	0.553	7.2	0.349	14.0	0.345
2.3	0.496	7.4	0.355	14.2	0.345
2.4	0.475	7.6	0.360	14.4	0.344
2.5	0.454	7.8	0.366	14.6	0.342
2.6	0.435	8.0	0.375	14.8	0.339
2.7	0.398	8.2	0.380	15.0	0.335
2.8	0.374	8.4	0.382	15.2	0.332
2.9	0.348	8.6	0.381	15.4	0.330
3.0	0.337	8.8	0.375	15.6	0.327
3.1	0.328	9.0	0.374	15.8	0.323
3.2	0.311	9.2	0.370	16.0	0.318
3.3	0.306	9.4	0.368	16.2	0.315
3.4	0.313	9.6	0.367	16.4	0.310
3.5	0.319	9.8	0.362	16.6	0.307
3.6	0.320	10.0	0.350	16.8	0.307
3.7	0.321	10.2	0.342	17.0	0.306
3.8	0.319	10.4	0.338	17.2	0.307
3.9	0.318	10.6	0.333	17.4	0.312
4.0	0.317	10.8	0.327	17.6	0.313
4.2	0.315	11.0	0.323	17.8	0.318
4.4	0.306	11.2	0.320	18.0	0.318
4.6	0.300	11.4	0.320	18.2	0.318

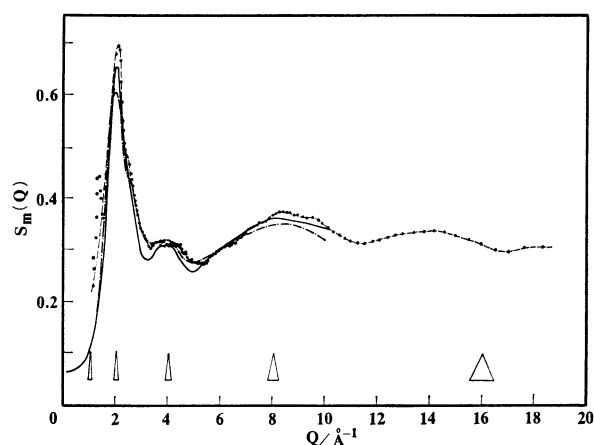


Fig. 4. The observed structure factors.

—●—: $S_m(Q)$ by the authors, (17 °C), ———: $S_m(Q)$ by Narten, (25 °C), ----: $S_m(Q)$ by Page and Powles, (22 °C).

curves: the curve A (fully corrected structure factor) and the curve B (the background correction only). The difference between two curves shows the effect of the multiple scattering, the absorption and the Placzek correction. The absolute structure factor, $S_m(Q)$ for liquid D₂O thus determined after all corrections and calibration is tabulated in Table 2, and shown again in Fig. 4, together with the factors given by Page and Powles and by Narten for comparison.

Analysis of Neutron Diffraction Data

i) *The Method of Analysis.* It is well known that strong orientational correlations are present between adjacent water molecules in liquid water. Then, we will analyze the present data using a model in line with the correlated orientation model³⁾ with respect to the nearest neighbor configuration of molecules.

Firstly, under the assumption that the relative orientation of pairs of molecules is correlated in a way which is independent of molecular separation,¹⁴⁾ the structure factor $S_m(Q)$ becomes³⁾

$$S_m(Q) = f_1(Q) + f_{2c}(Q)[S_c(Q) - 1], \quad (3)$$

where $f_1(Q)$ and $S_c(Q)$ are the intramolecular contribution and the molecular-centre structure factor, respectively. $f_{2c}(Q)$ is a factor resulting from the orientational configuration between neighboring molecules.

Here we consider what we call the "revised watery model," that is, a revised model originating from the "watery model" proposed first by Page and Powles.³⁾ In the model the relative orientation of adjacent

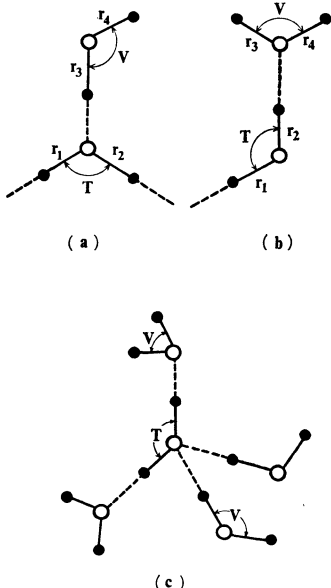


Fig. 5. The structure of the "revised watery model."

●: Deuteron nucleus, ○: oxygen nucleus.

Two types of hydrogen-bonded pairs between the central molecule and the peripheral one in the tetrahedral star-pentamer, (a): r_1 , r_2 , and $r_3=1.01 \text{ \AA}$, $r_4=0.96 \text{ \AA}$, (b): r_1 and $r_2=1.01 \text{ \AA}$, r_3 and $r_4=0.96 \text{ \AA}$. (c): the configuration of the tetrahedral coordination.

The four hydrogen-bonded molecules are rotating freely about each O-D...O axis. $V=104.5^\circ$, $T=109.5^\circ$.

molecules is shown in Fig. 5. The water molecules constituting the tetrahedral pentamer (Fig. 5) are classified into three groups according to the manner of hydrogen-bonding: 1) a central molecule in which two OD bonds are hydrogen-bonded (Fig. 5(c)), 2) two molecules in which one OD bond is hydrogen-bonded (Fig. 5(a)), and 3) two molecules in which two OD bonds are free (Fig. 5(b)). The non-hydrogen-bonded bond length r_{OD} is 0.96 Å (the length of the bond in the vapor molecule) and the hydrogen-bonded bond length r_{OD} 1.01 Å (the length of the bond in heavy ice I). The separation r_{OO} for hydrogen bond O-D...O is taken to be 2.82 Å.¹⁵⁾

The structure factor for heavy water is calculated by means of Eq. 3. The intramolecular contribution, $f_1(Q)$, consists of three varieties of factors (Fig. 5) for 1)—3) described above, and the intermolecular contribution is $f_{2c}(Q)[S_c(Q)-1]$, where the factor, $f_{2c}(Q)$, is the sum of two terms as the following equation:

$$f_{2c}(Q) = \frac{1}{2}[f_{2c}^a(Q) + f_{2c}^b(Q)]. \quad (4)$$

$f_{2c}^a(Q)$ and $f_{2c}^b(Q)$ are the structure factor for the configurations (a) and (b) in Fig. 5, respectively. These two are expressed as

$$\begin{aligned} f_{2c}^a(Q) = & [b_0^2 + b_0 b_D \{3j_0(Qr_{OD}^b) \exp(-\gamma_{OD}^b Q^2) \\ & + j_0(Qr_{OD}^v) \exp(-\gamma_{OD}^v Q^2)\} \\ & + 2b_D^2 \{j_0(Qr_s) \exp(-\gamma_s Q^2) + L(Q)\}] / \\ & (b_0 + 2b_D)^2, \end{aligned} \quad (5)$$

and

$$\begin{aligned} f_{2c}^b(Q) = & [b_0^2 + 2b_0 b_D \{j_0(Qr_{OD}^b) \exp(-\gamma_{OD}^b Q^2) \\ & + j_0(Qr_{OD}^v) \exp(-\gamma_{OD}^v Q^2)\} \\ & + 2b_D^2 \{j_0(Qr_p) \exp(-\gamma_{r,p} Q^2) + M(Q)\}] / \\ & (b_0 + 2b_D)^2, \end{aligned} \quad (6)$$

where

$$j_0(Qr) = \frac{\sin Qr}{Qr}, \quad (7)$$

$$L(Q) = \frac{1}{\pi} \int_0^\pi j_0[Qh_L(\xi)] \exp(-\gamma_{h,L} Q^2) d\xi, \quad (8)$$

$$M(Q) = \frac{1}{\pi} \int_0^\pi j_0[Qh_M(\xi)] \exp(-\gamma_{h,M} Q^2) d\xi, \quad (9)$$

$$h_L(\xi) = \left[r_{OD}^b{}^2 + r_{OD}^v{}^2 + \frac{2}{3} r_{OD}^b r_{OD}^v \{ \cos(\pi - V) \right. \\ \left. - 2\sqrt{2} \cos \xi \sin(\pi - V) \} \right]^{1/2}, \quad (10)$$

$$h_M(\xi) = \left[r_{OD}^b{}^2 + r_{OD}^v{}^2 + \frac{2}{3} r_{OD}^b r_{OD}^v \left\{ \cos \left(\frac{V}{2} \right) \right. \right. \\ \left. \left. - 2\sqrt{2} \cos \xi \sin \left(\frac{V}{2} \right) \right\} \right]^{1/2}, \quad (11)$$

$$r_p = 2 \left[r_{OD}^v{}^2 + \left(\frac{p}{2} \right)^2 - r_{OD}^v p \cos \delta \right]^{1/2}, \quad (12)$$

$$\delta = \cos^{-1} [(r_{OD}^v{}^2 + p^2 - r_{OD}^b{}^2)/2r_{OD}^v p], \quad (13)$$

$$p = [r_{OD}^b{}^2 + r_{OD}^v{}^2 - 2r_{OD}^b r_{OD}^v \cos T]^{1/2}, \quad (14)$$

and

$$r_s = 2r_{OD}^b \cos \left(\frac{T}{2} \right). \quad (15)$$

$b_0=0.577 \times 10^{-12}$ cm and $b_p=0.67 \times 10^{-12}$ cm are the coherent scattering length for oxygen and deuteron, respectively. The intramolecular oxygen-to-deuteron distance r_{OD}^i is the length of the O—D bond in heavy ice I and r_{OD}^v that in the vapor. $2\gamma_{OD}^i$, $2\gamma_{OD}^v$, $2\gamma_{h,L}$, $2\gamma_{h,M}$, $2\gamma_s$, and $2\gamma_{r,p}$ are the mean-square variation to the distance r_{OD}^i , r_{OD}^v , $h_L(\xi)$, $h_M(\xi)$, r_s , and r_p , respectively, and their magnitudes are known from various sources.^{16,17} The variation is assumed to be proportional to the corresponding bond length,¹⁸ being taken to be 0.06 Å per 1 Å for bond length. $V=104.5^\circ$ is the DOD angle for the molecule in the vapor and T the tetrahedral angle. ξ is the average rotational angle in relation to the average of the intermolecular distance r_{DD} .¹⁹ The molecular-centre structure factor, $S_c(Q)$, is obtained from X-ray scattering data.¹⁶

ii) *Results and Comparison with Previous Works.*

The structure factor $S_m(Q)$ for the "revised watery model," which has been calculated using Eqs. 3—15 is

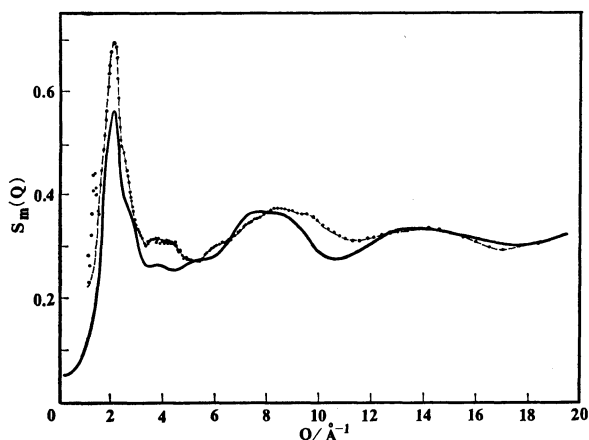


Fig. 6. The comparison between the calculated $S_m(Q)$ values for the "revised watery model" and the observed ones.

—: The calculated $S_m(Q)$ for the "revised watery model," -●-: the observed $S_m(Q)$.

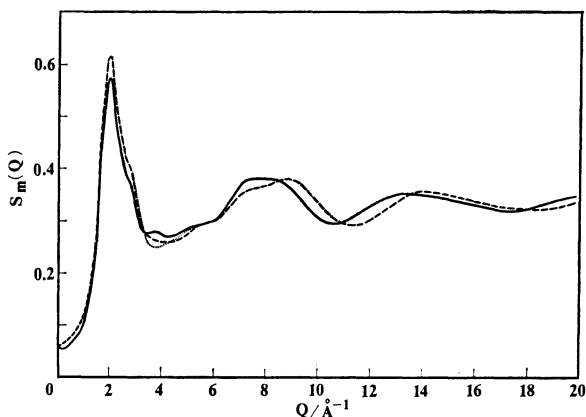


Fig. 7. The comparison between the calculated curve of $S_m(Q)$ for the "revised watery model" and the curves for other models.

—: $S_m(Q)$ for the "revised watery model," - - -: $S_m(Q)$ for the "watery model,": $S_m(Q)$ for the "uncorrelated orientation model."

given in Fig. 6 and compared with the experimental $S_m(Q)$ (Table 2, Fig. 4). The comparison with the calculated $S_m(Q)$ for other models is shown in Fig. 7; the "uncorrelated orientation model" and the "watery model" (Page and Powles).³ The agreement between calculated and experimental $S_m(Q)$ is not satisfactory as seen in Fig. 6 but slightly improved in comparison with other models as seen in Fig. 7.

Three experimental curves, which have been given by Page and Powles, by Narten and by the authors, are compared in Fig. 4. The main features of the curves consist of the largest peak at 2 \AA^{-1} , a bump about 4 \AA^{-1} and a broad peak ranging over 7 — 10 \AA^{-1} , including a rather smaller but clear shoulder at 2.8 \AA^{-1} . The absolute magnitude of these peaks may be regarded as being possessed of some uncertainties, taking into consideration the fact that a certain arbitrariness is present in the application of various kinds of corrections, for example, the assignment of M_{eff} in the Placzek correction etc. However, the position of the peaks and shoulder is unchanged at all before and after applying the corrections, as clearly seen in Fig. 3. In analyzing the data we must take into consideration these facts. From Figs. 3, 4, 6, and 7, it can be said that the behavior of curves near 4 \AA^{-1} is important in judging the adequacy of the model proposed, which has been noted by Page and Powles.³ Our model as well as others given in Fig. 7 is not successful in this respect, though our curve is somewhat improved.

The disagreement of the first peak which is seen in Fig. 6 is attributed to the ignorance of some long range order with the period of about 3 Å, probably. This may be ascribed to the presence of unbonded water molecules which is practically ignored in the present model as well as in Page and Powles' models (except the "uncorrelated orientation model") and Narten's model, considering the fact that the first peak is the highest in the "uncorrelated orientation model" (Page and Powles). In order to improve that we must use a mixture model,²⁰ which is impossible without introducing some adjustable parameters in the analysis.

Narten calculated $S_m(Q)$ according to his near-neighbor model,^{4,21} where one oxygen atom as an

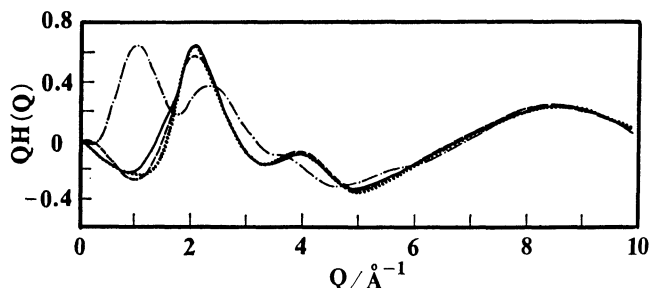


Fig. 8. The weighted structure function $QH(Q)$ calculated for Narten's model.

.....: The observed curve by Narten, ----: the calculated curve by Narten, —: the calculated curve by the authors for all $r_{\alpha\beta}=3 \text{ \AA}$, - - -: the calculated curve by the authors for all $r_{\alpha\beta}=5 \text{ \AA}$.

$H(Q)=S_m(Q)-\sum_{n=1}^3 b_n^2/(\sum_{n=1}^3 b_n)^2$, ($H(Q)$ is Eq. 10 in Ref. 4).

origin is surrounded by four other oxygens at the corners of a regular tetrahedron like Fig. 5 (c) and the region beyond the discrete structure is regarded as a uniform distribution of atoms, and obtained a very good fit with his experimental curve as shown in Fig. 8 which has been reprinted from his paper.⁴⁾ In order to investigate the nature of Narten's model, we have attempted to reproduce the calculation of $S_m(Q)$ according to the same procedures as described in that text, using quite identical values for molecular parameters except those for $r_{\alpha\beta}$.²²⁾ We have obtained the best curve for the assignment that all $r_{\alpha\beta} \equiv 3 \text{ \AA} = r_c$, which are the separation between the nucleus α in the central molecule and the nucleus β in the continuum region. The magnitude of $r_{\alpha\beta} \approx 3 \text{ \AA}$ is clearly too small. It should be larger than 4.5 \AA , considering the size of the discrete structure. When the larger values than 3 \AA are assigned to any of $r_{\alpha\beta}$, the shape and features of the $QH(Q) \text{ vs. } Q$ curve are found to vary and the good fit is quite missed. Then, it is concluded for Narten's model that the assignment of implausibly small values to the parameter $r_{\alpha\beta}$ is needed for obtaining the fit to the experimental data, and, otherwise it is not attained. Thus, the success reported in his paper⁴⁾ has turned out to be only apparent.

The authors are grateful to Associate Professor Takaaki Matsumoto and Mr. Masanobu Senda of Faculty of Engineering, Hokkaido University for their kindful cooperation in carrying out the experiment.

References

- 1) B. N. Brockhouse, *Nuovo Cimento Suppl.*, **9**, 45 (1958).
- 2) T. Springer, C. Hofmeyer, S. Kornblicher, and H. D. Lemmel, *Proc. Intern. Conf. on Peaceful Uses of Atomic Energy*, 3rd, Geneva (1964), Vol. 2, p. 351.
- 3) D. I. Page and J. G. Powles, *Mol. Phys.*, **21**, 901 (1971).
- 4) A. H. Narten, *J. Chem. Phys.*, **56**, 5681 (1972).
- 5) G. Walford, J. H. Clarke and J. C. Dore, *Mol. Phys.*, **33**, 25 (1977).
- 6) J. G. Powles, *Mol. Phys.*, **26**, 1325 (1973).
- 7) Y. Ishikawa and N. Watanabe, *Butsuri*, **28**, 461 (1973).
- 8) R. N. Sinclair, D. A. G. Johnson, J. C. Dore, J. H. Clarke and A. C. Wright, *Nucl. Instr. and Meth.*, **117**, 445 (1974).
- 9) K. Inoue, N. Ohtomo, H. Iwasa, and Y. Kiyanagi, *J. Nucl. Sci. Technol.*, **11**, 228 (1974).
- 10) N. Ohtomo and K. Inoue, *Bull. Fac. Eng. Hokkaido Univ.*, **73**, 105 (1974); *J. Nucl. Sci. Technol.*, **12**, 384 (1975); K. Inoue and N. Ohtomo, *J. Nucl. Sci. Technol.*, **13**, 389 (1976).
- 11) I. A. Blech and B. L. Averbach, *Phys. Rev.*, **137**, A1113 (1965).
- 12) H. H. Paalman and C. J. Pings, *J. Appl. Phys.*, **33**, 2635 (1962).
- 13) A. K. Soper, G. W. Neilson, J. E. Enderby, and R. A. Howe, *J. Phys. C: Solid State Phys.*, **10**, 1793 (1977).
- 14) J. G. Powles, *Adv. in Phys.*, **22**, 1 (1973).
- 15) K. Arakawa, K. Tokiwano, and K. Kojima, *Bull. Chem. Soc. Jpn.*, **50**, 65 (1977).
- 16) A. H. Narten and H. A. Levy, *J. Chem. Phys.*, **55**, 2263 (1971).
- 17) W. S. Benedict, N. Gilar and E. K. Plyler, *J. Chem. Phys.*, **24**, 1139 (1956); S. Shibata and L. S. Bartell, *J. Chem. Phys.*, **42**, 1147 (1965); W. C. Ermler and C. W. Kern, *J. Chem. Phys.*, **55**, 4851 (1971).
- 18) A. H. Narten, M. D. Danford, and H. A. Levy, *Discuss. Faraday Soc.*, **43**, 97 (1967).
- 19) In the paper of Page and Powles, this average angle ξ is represented by the notation ν defined in Eqs. 12 and 13 in Ref. 3.
- 20) K. Arakawa, *Kagaku Sosetsu*, No. 11, 35 (1976).
- 21) A. H. Narten, M. D. Danford, and H. A. Levy, *J. Chem. Phys.*, **46**, 4875 (1967); A. H. Narten and H. A. Levy, *Science*, **165**, 447 (1969).
- 22) The OD and DD distances and their rms variations $(2\gamma)^{1/2}$ are taken to be

$$r_{OD} = 0.934 \text{ \AA}, \quad (2\gamma_{OD})^{1/2} = 0.138 \text{ \AA},$$

$$r_{DD} = 1.53 \text{ \AA}, \quad (2\gamma_{DD})^{1/2} = 0.24 \text{ \AA},$$
according to Ref. 4.